de Haas−van Alphen measurements of the electronic structure of LaSb₂

R. G. Goodrich,[1] D. Browne,[1] R. Kurtz,[1] D. P. Young,[1] J. F. DiTusa,[1] P. W. Adams,[1] and D. Hall[2,*]

[1]*Department of Physics and Astronomy, Louisiana State University, Baton Rouge, Louisiana 70809, USA*
[2]*National High Magnetic Field Laboratory, Florida State University, Tallahassee, Florida 32306, USA*

We report the results of de Haas−van Alphen measurements in high magnetic fields on the anisotropic compound LaSb₂. Our measurements reveal three extremal orbits of the Fermi surface. One is very small and ellipsoidal, while the remaining two are larger and have a nearly cylindrical shape indicating a quasi-two-dimensional Fermi surface. We compare these measurements with the results of energy band calculations and find reasonable agreement with the measured Fermi surface areas, though the calculations show other multi-connected regions of the Fermi surface not observed in the de Haas−van Alphen spectra. The implications of our calculated and measured Fermi surfaces on the mechanisms proposed for the extraordinary large linear magnetoresistance in LaSb₂ are discussed.

INTRODUCTION

Materials that exhibit a large magnetoresistance (MR) have received a great deal of attention in the past decade because of their potential use as magnetic field sensors in read-write heads.[1] Magnetic materials often are employed in MR devices by exploiting the field sensitivity of interface scattering between layers of magnetic-nonmagnetic films. Also, suppressing magnetic fluctuations in a magnetic conductor can decrease carrier scattering and results in a large MR.[2–5] There also are several notable examples of materials in which large MRs result from the Coulomb interactions between carriers.[6–8] Most intriguing are materials in which no suitable mechanism is known for the large MR. The last group includes AgSe₂ (Refs. 9 and 10) and the rare earth diantimonides in which large linear field dependent resistivities have been measured over wide ranges of magnetic field. The nonmagnetic member of this latter group is the metal LaSb₂, which exhibits a large linear magnetoresistance with no sign of saturation up to fields of 45 T.[11] Both the size of the positive MR (10 000%) (Ref. 11) and its linear form are surprisingly at odds with the standard semi-classical theory[12] of MR. This theory of band structure effects on the transport properties of metals predicts a resistance that increases quadratically with magnetic field. The exception is for materials with open Fermi surface (FS) orbits, in which case the MR eventually saturates.

Because of the obvious failure of the semiclassical models, several mechanisms have been suggested that are successful in producing a linearlike MR over small ranges of magnetic field. These rely on either magnetic breakdown effects in charge density wave (CDW) materials,[13] local fluctuations in carrier density,[14] high field quantization effects,[15] or macroscopic disorder and strong inhomogeneities in semiconductors.[10] The quantization and carrier density fluctuation effects are predicted to be measurable only in the restricted case of very low carrier concentrations in extremely high mobility samples. Neither of these restrictions appear to be met in our LaSb₂ crystals. We will show that LaSb₂ displays quantum oscillations in its magnetization, ruling out most sources of inhomogeneity and disorder as a

mechanism for MR. On the other hand, LaSb₂, and the other rare earth diantimonides, have anisotropic two-dimensional-like crystal structures similar to the classic CDW compounds NbSe₂ and TaSe₂, both of which display large linear MRs. However, no CDW ground state has been established for LaSb₂.

In this paper we report the results of de Haas−van Alphen (dHvA) measurements on LaSb₂ and compare them with our energy band calculations and calculated FS areas for the known structure of LaSb₂.[16] We find agreement between the three measured FS areas and three of the areas from the calculation. Our measurements indicate that, if a CDW ordering occurs in this material, it affects neither the pieces of the Fermi surface near the zone center nor those parts near the zone boundaries at the *S* point of the orthorhombic Brilloiun zone. CDW phases are generally thought to occur in highly nested Fermi surfaces. The simplest nesting evident in our band structure calculations involves pieces of the Fermi surface that are not observed in our measurements. Although there is no evidence of a CDW instability, our data are consistent with such a conjecture and do not rule out the existence of a CDW ground state in LaSb₂.

EXPERIMENTAL PROCEDURE

LaSb₂ is a member of the *R*Sb₂ (*R*=La-Nd, Sm) family of compounds that all form in the orthorhombic SmSb₂ structure.[16] It is comprised of alternating La/Sb layers and two-dimensional rectangular sheets of Sb atoms stacked along the *c* axis. Similar structural characteristics give rise to the anisotropic physical properties observed in all the compounds in the *R*Sb₂ series.[17] We have chosen to investigate LaSb₂ since it is nonmagnetic and, thus, its low-temperature properties are not complicated by magnetic phase transitions that occur in the other rare earth diantimonides.[5] Single crystals of LaSb₂ were grown from high purity La and Sb by the metallic flux method.[18] The structure and quality of these crystals has been reported previously.[11]

Measurements of the de Haas−van Alphen effect were made between 1.5 and 15 K in magnetic fields *B* between 20 and 45 T at the National High Magnetic Field Laboratory,
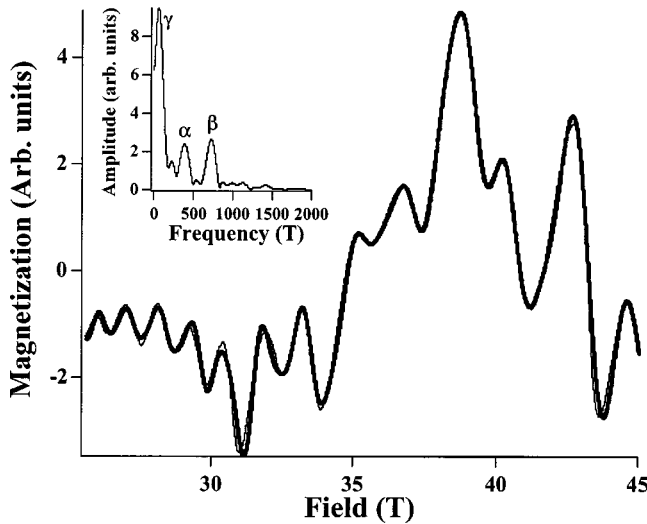
FIG. 1. Magnetization as a function of field (solid line) of $LaSb_2$ at 6 K. The dotted line is a fit to the data for the three frequencies shown in the Fourier transform of the data in the inset.

FIG. 2. Angular dependence of three dHvA frequencies for rotations from $0°$ at $B\|[001]$ toward $B\|[100]$ at $90°$.

Tallahassee, FL. The sample torque magnetization was measured using a rotatable cantilever system that allows data to be recorded as a function of the crystal orientation with respect to the applied magnetic field in $5°$ steps over a $90°$ angular range in the a-c plane. In addition, effective mass measurements were made near $B\|[001]$ from the temperature dependence of the dHvA signals between 1.5 and 10 K.

RESULTS

In Fig. 1 a typical dHvA data set is displayed, taken at 6 K with the crystal c axis $2.5°$ from the magnetic field direction. Clear oscillations of the magnetization are visible in the raw data. The Fourier transform of those data, shown in the inset, reveal that these oscillations result from three independent frequencies in $1/B$, indicating three extremal Fermi surface areas. The observed low frequencies limit the number of oscillations falling within our field range. Therefore, to determine the frequencies more accurately we performed a fit of the Lifshitz–Kosevitch (LK) equation[19] to our data. The result of the fit using three independent frequencies is shown by a dotted line in Fig. 1. As can be seen from the quality of the overall fit, constant frequencies are observed up to 45 T with no changes in the various Fermi surface sizes or shapes. The two highest frequencies obtained from the fit are in agreement ($\square$ 2%) with those determined from the Fourier analysis. However, the lowest frequency from the fit differs considerably from that determined using the Fourier transform. By inspection of the data, it can be seen that there are at most 1.5 oscillations of this low frequency in the field range of 20–45 T, and therefore the Fourier transform is not reliable. In the analysis that follows we have used the frequencies obtained from the LK fits for the low frequency since they are a more reliable measure of this oscillation frequency than the peak in the Fourier transform spectrum.

We have measured the variation in these three frequencies as a function of angle between the crystallographic axes and
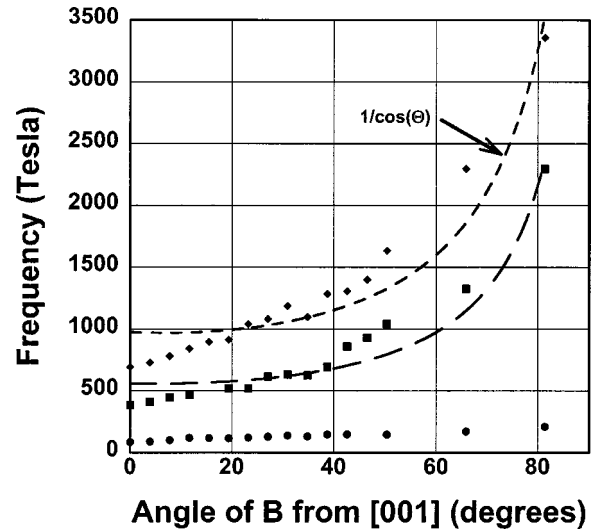
the applied field to fully exploit the de Haas–van Alphen technique. The orientation of the crystal [001] axis was varied from a position parallel to B to one in which it is perpendicular to B along the [100] axis. The changes in the frequency of the magnetization oscillations with rotation gives a sense of the Fermi surface shape, which we expect to be highly anisotropic due to the planar crystal structure of this compound. We were able to identify oscillations of the magnetization at measurement angles of B with respect to the axis direction between $-10°$ and $100°$, except near $90°$. For several orientations of the [001] axis with respect to the magnetic field direction we found agreement between the frequencies determined from the Fourier analysis and the fits of LK theory for the two higher of the three frequencies. This gives us confidence in our analysis over the entire angular range of rotation.

In Fig. 2 the angular dependences of the three frequencies are displayed, showing that our expectations of anisotropy were met by two of the three Fermi surface extremal areas. At angles having the applied field between $85°$ and $95°$ from the [001] axis neither of the higher frequency signals were observed, but they reappeared for angles greater than $100°$ with decreasing frequency as the angle was increased. In addition, the data are symmetrical around $B\|[001]$. For comparison we have plotted a $1/\cos(\theta)$ dependence, where θ is the angle between the applied field and the [001] axis. The dashed lines in the figure represent this $1/\cos(\theta)$ angular dependence that would occur for a perfectly cylindrical Fermi surface. The similar angular dependent form of our data indicates that these Fermi surface pieces are indeed open in the [001] direction, as would be the case for a two-dimensional surface. We conclude that these two Fermi surface pieces both are connected along the Γ-Γ direction in the Brillouin zone (BZ) and are roughly cylindrical in shape. In contrast, the smallest frequency signal is shown by both analysis methods to be only slightly angular independent, indicating a small nearly spherical pocket of Fermi surface.

The de Haas–van Alphen technique also allows one to

measure carrier masses via the temperature dependence of the magnetization oscillation amplitude.[19] We have measured the temperature dependence of the oscillation amplitudes from 1.5 to 10 K using the Fourier transform of the dHvA signals. A crystalline orientation with the [001] axis 15° from the magnetic field direction was chosen to maximize the amplitude of the oscillations evident in the cantilever signal. The reduction in these amplitudes with temperature defines the effective masses of the two higher frequencies to be $m^* = 0.22$ for the 393-T oscillation and $m^* = 0.17$ for the 729-T oscillation. All three of the signals were clearly observable up to 10 K, indicative of the light masses. The mass of the lowest frequency, γ, was not obtained.

The picture of the LaSb$_2$ electronic structure that emerges has at least three Fermi surface pieces, two of which have two-dimensional characteristics, and the third, smaller piece, being three dimensional. All of these Fermi surface areas are relatively small, which indicates that there are few itinerant carriers in this compound. This conclusion is consistent with Hall effect measurements of the carrier density that indicated a hole density of 3.0×10^{20} cm^{-3} and a mobility of 500 cm^2/Vs[11].

ENERGY BAND CALCULATIONS

In order to understand the electronic structure of this compound more fully, we have performed energy band calculations of LaSb$_2$.[20] These band calculations employed the WIEN2K software package,[21] which implements a full potential all-electron linear augmented plane wave (LAPW) density functional calculation using the correlation potentials of Perdew et al.[22] The spin-orbit interaction for the valence and semi-core states was included perturbatively. The La and Sb muffin tin radii were set at 2.85 and 2.65 a.u. respectively. A plane-wave cutoff of 5 a.u.$^{-1}$ was employed, resulting in a total of 649 plane waves. Semicore states for La s and p and Sb s and d states were included with 216 local orbitals, and a total of 144 k points were kept in the irreducible Brillouin zone while iterating to self-consistency. After the calculation had converged, a much finer grid of $81 \times 81 \times 11$ points in the irreducible wedge was employed to calculate the FS. Cross sections of the overall FS obtained from these calculations in the $\Gamma Y_1 Y_2$ plane (zone center) are shown in Fig. 3 in the repeated zone scheme.

We have listed the theoretical and experimental frequencies in Table I and associate the three observed frequencies for $B \| [001]$ with the three FS orbits marked α, β, and γ in Fig. 3. For the smallest orbits in Fig. 3, γ and β', the band calculation is the least accurate because the grid would have to be much finer to obtain accurate results. It may be possible that in a more accurate calculation the Fermi level would shift enough to remove the β' feature entirely. As can be seen, the agreement for α (16%) and β (7%) is reasonable while the agreement for γ is not as accurate, but as noted above the experimental frequency was difficult to determine, and the calculation the least accurate for this orbit.

The angular dependence seen experimentally is also consistent with the topology of the calculated Fermi surfaces. The orbits marked α and β are associated with sheets that are

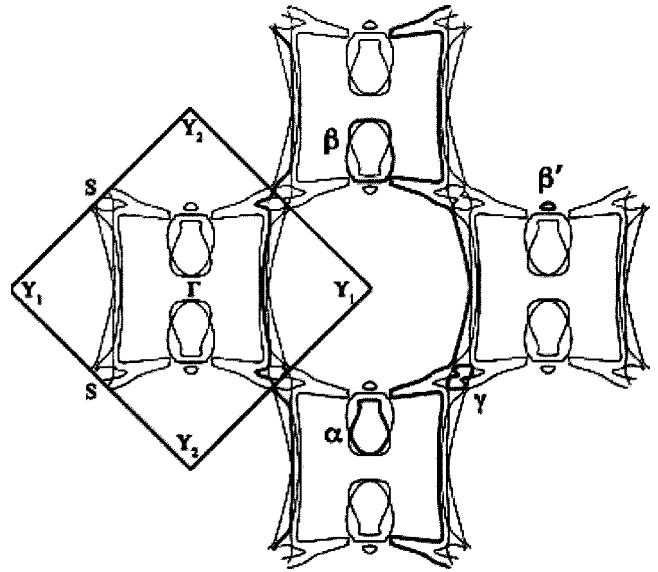FIG. 3. Fermi surface contours in the extended zone scheme with each of the closed orbits for $B \| [001]$ highlighted and two different open orbits in the $\Gamma Y_1 Y_2$ plane highlighted. Also shown are the boundaries of the first BZ with symmetry points (Bilbao Crystallographic Server at http://www.cryst.ehu.es) indicated.

rather two dimensional, having open orbits along the [001] axis, and show a rather small (10%) variation in cross section along the [001] direction, which is consistent with the experimental angular dependence seen for the two higher frequency components. The orbit marked γ is a small three-dimensional electron pocket centered at the S point. The frequency (64 T) is similar to the lowest component observed (102 T), whose variation with angle is consistent with the experimental behavior. There are two other large pieces of the FS in the $\Gamma Y_1 Y_2$ plane arising out of the energy band calculations that result in open orbits in the plane perpendicular to the [001] axis. These open orbits also are highlighted in Fig. 3, and because they are open orbits at all measured angles they cannot be observed.

DISCUSSION AND CONCLUSIONS

If a CDW exists at low temperatures, the nesting of the wave vector should be most prominent along the sheets of the Fermi surface that produce the experimentally unobserved open orbits in Fig. 3. We would expect those parts of the FS to be removed by the formation of the CDW gap. On the other hand, the parts of the FS located near the high symmetry points in the zone giving rise to the α and β orbits,

TABLE I. Calculated and measured dHvA frequencies for the magnetic field applied along the [001] axis in LaSb$_2$.

Orbit	Calculated (T)	Experiment (T)
α	457	393
β	780	729
β'	22	Not Observed
γ	64	102

would be unaffected by the presence of a CDW that formed due to nesting between the open orbit sheets. In Ref. 20 the nesting between branches of these parts of the FS that would lead to CDW formation is discussed in detail. In addition, the calculated FS volumes and effective masses are given in Ref. 20.

In summary, we have measured de Haas–van Alphen oscillations in $LaSb_2$ as a function of magnetic field, temperature, and crystal orientation. From these measurements we have observed three small Fermi surface sheets, two of which are nearly cylindrical about the [001] direction of the Brillouin zone, and a smaller third sheet, which is nearly spherical. The areas of the cylindrical Fermi surfaces are small, leading to the conclusion, consistent with our transport data, that $LaSb_2$ has a small number of itinerant carriers. Our band structure calculations reveal five Fermi surface sheets, three having areas that are in quantitative agreement with our measurements, while the two remaining give rise to open orbits not observable in this experiment. Our measurements of the carrier masses, combined with our earlier estimate of the carrier density effectively rule out any quantization effects as the cause of the linear MR. Such theories rely on extremely small carrier densities and very large Hall mobilities, neither of which are supported by our data. Furthermore, the observation of de Haas-van Alphen oscillations effectively rules out the usual routes to macroscopic disorder necessary for to explain large MRs in disordered semiconductors.[10] Although no direct evidence for a CDW instability has been reported, our band structure calculations are consistent with such a hypothesis. If such a CDW state forms the pinning of CDW modes at impurity sites may provide the inhomogeneity required by one of the theories for large linear MRs.[10]

*Present address: American Physical Society, One Research Road, Box 9000, Ridge, New York 11961, USA.

[1] G. A. Prinz, Phys. Today **48** (4), 58 (1995).

[2] C. W. Searle and S. T. Wang, Can. J. Phys. **47**, 2703 (1969).

[3] S. Jin *et al.*, Science **264**, 413 (1994).

[4] Y. Tokura *et al.*, J. Appl. Phys. **79**, 5288 (1996).

[5] Y. Shimakawa, Y. Kubo, and T. Manako, Nature (London) **379**, 53 (1996).

[6] N. Manyala, S. Sidis, J. F. DiTusa, G. Aeppli, D. P. Young, and Z. Fisk, Nature (London) **404**, 581 (2000).

[7] V. Yu. Butko, J. F. DiTusa, and P. W. Adams, Phys. Rev. Lett. **85**, 162 (2000).

[8] R. Xu, A. Husmann, T. F. Rosenbaum, N.-L Saboungi, J. E. Enderby, and P. B. Littlewood, Nature (London) **390**, 57 (1997).

[9] A. Usmann, J. B. Betts, G. S. Boebinger, A. Migliori, T. F. Rosenbaum, and L. Saboungi, Nature (London) **409**, 161 (2001).

[10] M. M. Parish and P. B. Littlewood, Nature (London) **426**, 162 (2003).

[11] D. P. Young, J. F. DiTusa, R. G. Goodrich, S. Guo, and P. W. Adams, Appl. Phys. Lett. **82**, 3713 (2003).

[12] See, e.g., N. W. Ashcroft and N. D. Mermin, *Solid State Physics* (Saunders, New York, 1976).

[13] J. A. Wilson, F. J. DiSalvo, and S. Mahajan, Adv. Phys. **24**, 117 (1975); A. H. Castro Neto, Phys. Rev. Lett. **86**, 4382 (2001).

[14] S. H. Simon and B. I. Halperin, Phys. Rev. Lett. **73**, 3278 (1994).

[15] R. A. Young, Phys. Rev. **175**, 813 (1968); A. A. Abrikosov, Phys. Rev. B **60**, 4231 (1999); A. A. Abrikosov, Europhys. Lett. **49**, 789 (2000); J. Phys. A **36**, 9119 (2003).

[16] F. Hullinger, in *Handbook of Physics and Chemistry of Rare Earths*, edited by K. A. Gschneidner and L. Eyring (North-Holland, Amsterdam, 1979), Vol. 4, p. 153.

[17] S. L. Bud'ko, P. C. Canfield, C. H. Mielke, and A. H. Lacerda, Phys. Rev. B **57**, 13 624 (1998).

[18] P. C. Canfield and Z. Fisk, Philos. Mag. B **65**, 1117 (1992).

[19] D. Shoenberg, *Magnetic Oscillations in Metals* (Cambridge University Press, Cambridge, 1984).

[20] D. Browne and R. Kurtz (unpublished).

[21] P. Blaha, K. Schwartz, G. K. H. Madsen, D. Kvasnicka, and J. Luitz, WIEN2K, An Augmented Plane Wave+Local Orbitals Program for Calculating Crystal Properties (Karlheinz Schwarz, Techn. Univ., Wien, Austria), 2001.

[22] J. P. Perdew, S. Burke, and M. Ernzerhof, Phys. Rev. Lett. **77**, 3865 (1996).